Available online at www.sciencedirect.com
ScienceDirect
Journal of Hazardous Materials 144 (2007) 687–691
Journal of Hazardous Materials
www.elsevier.com/locate/jhazmat

CFD methods for the reduction of reactive gas emission from a paper laminating machine

Andras Horvath [a], Christian Jordan [a], Gerhard Forstner [b], Peter Altacher [b], Michael Harasek [a,*]

[a] *Institute of Chemical Engineering, Getreidemarkt 9/166, 1060 Wien, Vienna University of Technology, Austria*
[b] *SIG Combibloc GmbH & Co. KG, Industriestrasse 3, 5760 Saalfelden, Austria*

Available online 30 January 2007

Abstract

In cooperation with the world's second largest manufacturer of beverage cartons (SIG Combibloc®) for liquid foodstuffs an innovative off-take for neutralisation of reactive gas in a paper laminating machine was constructed. A great challenge during engineering work was ensuring a high concentration of the reactive gas where needed and at the same time minimising work place impact in a machine basically without housing.

Preliminary 2D-models of the machine geometry proved to be insufficient in describing all the governing flow phenomena. A simplified 3D-geometry containing all important parts of the complex machinery was necessary for accurate predictions.

It was found that the driving force of air movement and transport of reactive gas (which acts as an adhesive agent) from the reaction zone in the interior of the laminating machine to the outside is a boundary flow caused by the rapid movement of carton material and rotating cylinders. A physically correct simulation result of the boundary flow is a premise for correct prediction of air flow in and around the machinery. Lacking experimental data (due to an inaccessible geometry) a worst case scenario was constructed by generating a grid and using turbulence models that maximised mass transport in the boundary layer region and thus emission of (tracer)gas from the machine. CFD simulations were done using the geometry preprocessor Gambit™, and the finite volume solver Fluent™.

The results of the analysis of the emission paths from the machine were surprising and led to the construction of an effective off-take relatively far away from the emission source. The chosen position ensures low disturbance of highly sensitive flow patterns inside the machine and diffusive mixing, dilution and contamination of the surroundings. The effect of the new off-take is an immediate and significant rise in air quality in the vicinity of the laminating machine and ensures maximum allowed concentration in the plant area. The product quality furthermore is uncompromised by the working off-take which was another important goal of this work.

Keywords: CFD; Emission; Boundary layer; Lamination; Packaging

1. Introduction

SIG Combibloc®, produces large amounts of laminated beverage cartons. The raw cartons have a width of 1.4 m and are produced at a speed of 8 m/s. Treatment of the used polymer-film with reactive gas is necessary to enhance adhesivity to the paper-base and to ensure mechanical stability of the compound material. Due to the open design of the laminating machines they are prone to emission problems caused by air movement and pressure gradients inside the laminator. The main factor of (unwanted) air flow inside the machine is the rapid movement of paper and its attached boundary flow. To understand flow phenomena and construct efficient off-takes it is necessary to correctly simulate the boundary flow.

1.1. Problem description

The production of cartons for liquid foodstuff implies the laminating of both sides of the carton and often the application of aluminium as additional barrier layer for oxygen diffusion. The various polymer films are produced in an extruder nozzle and immediately after contact with the carton cooled on a special roller. The carton is under constant tensile stress and has to be in contact with rollers approximately every meter of length to avoid uncontrolled oscillations of the carton surface.

The individual operations are performed by three different laminating machines. They are here described as types "A", "B"

* Corresponding author. Tel: +43 1 58801 15925; fax: +43 1 58801 15999.
E-mail address: michael.harasek@tuwien.ac.at (M. Harasek).

0304-3894/$ – see front matter © 2007 Elsevier B.V. All rights reserved.
doi:10.1016/j.jhazmat.2007.01.096

Nomenclature

C_μ	constant in k–ϵ-model
k_P	turbulent kinetic energy at point P
U_P	mean velocity of the fluid at point P
U^*	dimensionless velocity
$\partial v/\partial n$	normal velocity gradient
y_P	wall distance of cell centroid P
y^*	dimensionless wall distance

Greek letters

ϱ	fluid density
ϵ	turbulent dissipation rate
μ	dynamic fluid viscosity at P
ν	kinematic fluid viscosity
τ_ω	wall shear stress in laminar flow

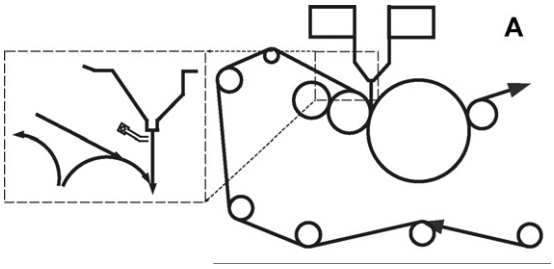

Fig. 1. Schematic plan of geometry type "A" with detail of reactive gas nozzle position (see enlargement on the left).

and "C". A schematic drawing of machine type "A" and is shown in Fig. 1. In the upper part of the schematic plan the extruder and off-takes for polymer fumes and reactive gas is shown. The rolling direction of the carton base is indicated by arrows. The rollers and distances are to scale. The ground level is indicated by a thin line in the bottom of the schematic drawing.

Reactive gas is applied in most cases at all three laminating machines. The nozzle for reactive gas is placed close to the polymer film at the extruder nozzle to guarantee high concentration levels and reaction rates on the polymer film.

The emission of reactive gas is unavoidable in an open design. The problem was to minimise concentration of reactive gas in the vicinity of the machine and ensure high concentrations at the polymer surface.

1.2. Strategies of solution

The first simulation runs were done with a 2D-geometry assuming negligible flow perpendicular to the grid-plane. This is however only valid in the center of the laminating machine. The emission and flow-characteristics cannot be implemented in a 2D-geometry, yet the simulation results yielded valuable information about flow patterns in the very center of the machine. It was further found that optimising the reactive-gas nozzle with regards to emission was impossible with a 2D-geometry.

A 3D-model of the innermost part of the laminator including a roller and the free space beneath the carton and the roller was constructed. The simulation results were surprising and showed the transport of reactive gas below the rollers where it was further diluted. The conclusion of these first simulation runs was that an implementation of the whole geometry (moving rollers, moving carton, off-takes, etc.) was necessary to track emission paths. The "pressure-outlet" boundary had to be far enough away from the emission source to include the vicinity of the machine.

All the moving parts should be implemented as moving walls with defined roughness. Boundary layers had to be attached to all moving walls and the resulting grid had to be feasibly small in RAM consumption. Prior to implementation the driving force of gas displacement (the moving walls with attached flow) was numerically studied in several 2D cases.

2. Preliminary numerical studies

The influence of grid-size and turbulence models on the steady-state boundary-flow of a flat moving wall with defined roughness were studied (see also) [1,2].

The following turbulence models were considered: realizable-k–ϵ (r-k–ϵ), shear-stress-transport- k–ω (sst-k–ω) and Reynolds-stress-model (RSM). For r-k–ϵ and RSM the influence of non-equilibrium wall-functions were studied.[1] An overview of a typical test case is shown in Fig. 2. The computational domain is 5 m × 0.5 m (31,500 finite volume cells), with the moving wall in the bottom and three pressure outlets.

Three different 2D-grids were constructed.

An important dimensionless number in CFD is y^*. For a cell centroid P the definition is as follows (also see [3]):

$$y^* = \frac{\varrho C_\mu^{1/4} k_P^{1/2} y_P}{\mu} \tag{1}$$

In the CFD package Fluent™, the laminar stress–strain relationship (when using standard wall functions) is applied to a wall-adjacent cell if $y^* < 11.225$ which can be written as $y^* = U^*$ where

$$U^* = \frac{U_P C_\mu^{1/4} k_P}{\tau_\omega/\varrho} \tag{2}$$

and

$$\tau_\omega = \mu \frac{\partial v}{\partial n} \tag{3}$$

In addition to the standard wall function described above (which is the default near-wall treatment in Fluent™) a two-layer-based non-equilibrium wall funtion is also available. The non-equilibrium wall function employs the two layer-concept in computing the budget of turbulence kinetic energy at the wall adjacent cells, which is needed to solve the k equation at the wall neighbouring cells. The wall-neighbouring cells are assumed to

[1] There is no selection of wall treatment possible in the sst-k–ω turbulence-model.

Fig. 2. Contour plot of absolute velocity above a moving wall (2D-simulation). Domain size: 5 m × 0.5 m. Speed of moving boundary: 8.33 m/s. Direction of movement: from right to left. At the white areas (top left and top right) the absolute velocity is less than 1% of the wall velocity.

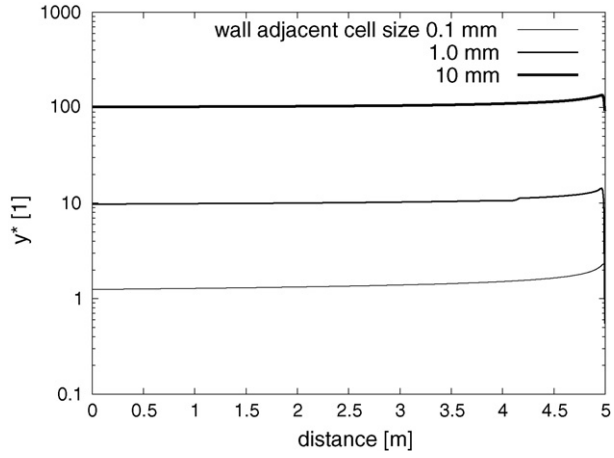

Fig. 3. Length of a moving wall and y^* of the wall-adjacent cell of the three considered grids. Simulation results based on k–ϵ-model with standard wall functions.

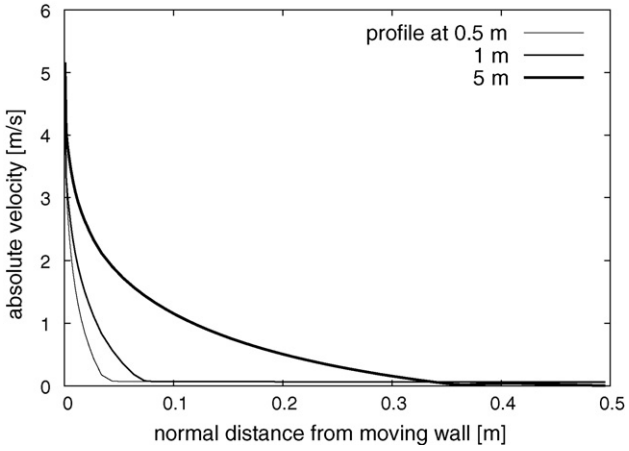

Fig. 4. Typical profiles of velocity along a flat moving wall (r- k–ϵ-turbulence model, non-equilibrium wall-functions, size of wall-adjacent cell: 1.0 mm, second order discretisation for all field variables).

consist of a viscous sublayer and a fully turbulent layer.[2] Because of the capability to partly account for the effect of pressure gradients and departure from equilibrium, the non-equilibrium wall functions are recommended for use in complex flows involving separation, reattachment and impingement where the mean flow and turbulence are subjected to severe pressure gradients and change rapidly.

For non-equilibrium wall functions profiling assumptions for the viscous sublayer are made by use of following equation:

$$y_v = 11.225 \cdot \frac{y_P}{y^*} \tag{4}$$

where y_v is the dimensional thickness of the viscous sub-layer and y is the distance from the wall.

If $y > y_v$ the properties are derived from the laminar stress strain relationship (like in standard wall functions). For other values of y the following equations apply for the turbulent-kinetic-energy k and the dissipation rate ϵ:

$$k = \left(\frac{y}{y_v}\right)^2 k_P, \qquad \epsilon = \frac{2\nu k}{y^2}$$

In Fig. 3, y^* is plotted against the length of a flat moving wall for the three considered grids. To guarantee that $y^* < 11.225$ for moving walls with mean velocity of 8.33 m/s that are shorter than 5 m the wall-adjacent cell must not exceed a thickness of 1 mm. If this criterion is met all the wall-adjacent cells are treated as described above. In other cases the cells are treated with different functions.[3] A cell size of 1 mm or less for the wall-adjacent cells should provide a sensible approach for the implementation of the 3D-geometry (both for standard and non-equilibrium wall functions). For small gaps and tapering lines an even smaller cell size is useful to avoid highly skewed/distorted cells.

The real flow patterns inside the machine were not accessible in experiments (without affecting the flow itself), so the idea was to implement a "worst case" model in which the mass transport of the boundary flow was maximised. This would cause maximal transport and emission of reactive gas in the simulation. An off-take constructed for the simulated worst case should work well in the real laminating machine.

The profiles of absolute velocity (at 0.5, 1 and 5 m length of the moving wall) were compared for all considered turbulence models and standard as well as non-equilibrium wall-functions for all considered grids (see exemplary Fig. 4).

It was found that the r-k–ϵ-turbulence model with non-equilibrium wall functions yielded the highest values for absolute velocity for all grid-sizes. This turbulence model was chosen for all further simulations. A comparison off cell-size effects is shown in Fig. 5. Considering the profound effect of the size of the wall-adjacent cell on velocity profiles and y^* a cell size of 0.25 mm for the wall-adjacent cell was chosen to implement the boundary layers in the 3D-grid.

[2] See also: Fluent™, 6.2.16 manual: 11.9.2 wall functions.

[3] For example: for standard wall-functions the log-law is applied for $30 < y^* < 300$. For the test case for cell size of 10 mm (see Fig. 3).

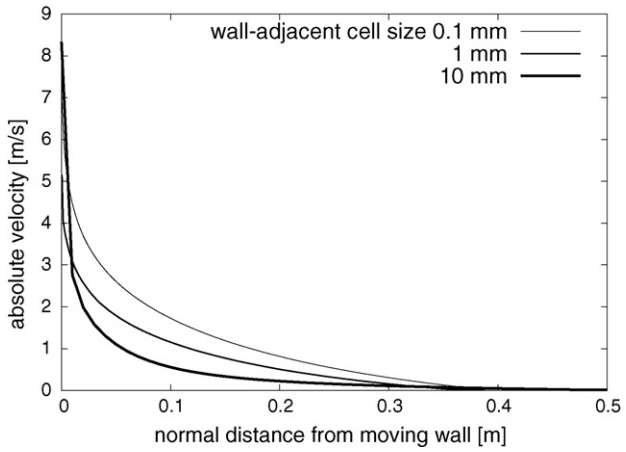

Fig. 5. Comparison of effect of cell size on velocity profile at 5 m (r- k–ϵ-turbulence model, non-equilibrium wall-functions, second order discretisation for all field variables).

3. Simulations and results

The laminating machines type A, B and C were implemented utilising from 1.4 to 1.6 million finite volume cells. Boundary layers as described above were applied to all moving parts. For the moving carton the boundary layers were applied on the upper and lower side of the paper. The diffusive and convective transport of reactive gas was implemented using Fluent's "species model" utilising actual gas properties. The grid fully consisted of unstructured hexahedral cells. All field variables were discretised with a second order scheme. Eleven surface monitors were used to watch reactive gas concentrations and freight to determine convergence of the steady state solver. Scripts were written for automatic meshing of the movable laminating nozzle with attached main off-takes. Effects of the position of the laminating nozzle on emission and flow patterns were simulated.

Fig. 6 gives an overwiev of the 3D-implementation of geometry "A" and Fig. 7 shows the main flow patterns that cause transport and dilution of reactive gas.

One of the most important results from the first 3D simulations was the observation of high freights (concentration times velocity) of reactive gas below the big roller which was rather unexpected. The conclusion was that an effective off-take could only be built at that position. All the three geometries showed similar flow patterns with the highest emissions close to the reactive gas nozzle and below the surface of the moving carton. The unmodified geometries had an average emission of 5% (referred to the total reactive gas input through the nozzle). The balance error of all simulations was in the order of 10%.

Table 1
Five-min average of measured reactive gas concentration at different measurement locations of laminating machine type "A" before and after installation of the new off-take

Position	Concentration (μg/ m^3)	
	Old off-take	New off-take
1	<20	20
2	90	20
3	40	25
4	50	15
5	20	15
6	40	20
7	80	25
8	400	70
9	180	50

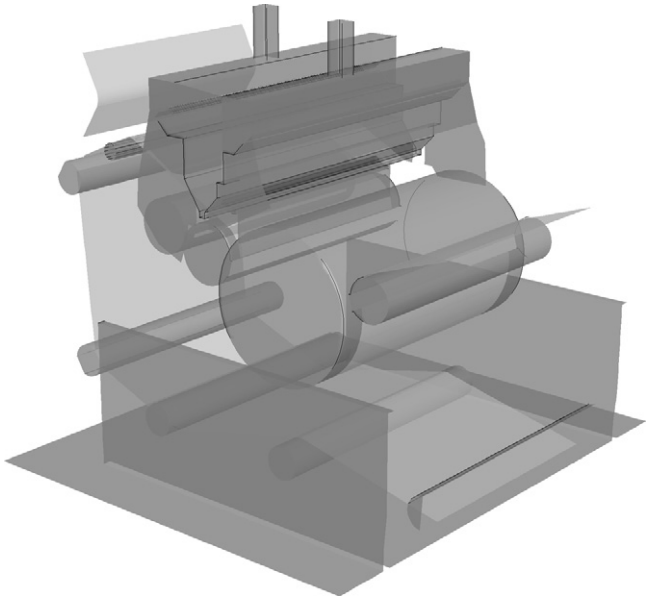

Fig. 6. Overview of 3D-implementation of laminating machine type "A" (unmodified geometry without new off-take). The geometry consists of 1.4 million finite-volume-cells.

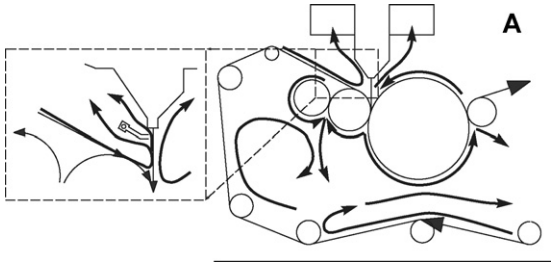

Fig. 7. Important flow patterns at the middle of the laminating machine type "A" (unmodified geometry without new off-take). Note the main off-takes at both sides of the laminating nozzle (see Fig. 6 for actual geometry).

To take advantage of the existing flow the new off-take was implemented below the big roller and close to it's rotating surface.

The simulation of the new off-take with optimised flow rate cut emission of reactive gas by half. A slightly modified construction was effective for all laminating machines. The overall emissions of all three laminating machines were reduced by 50%. The simulated results were confirmed by concentration measurements before and after the installation of the new off-take. The product quality was uncompromised by the new off-take.

4. Measurements

The measurements were conducted with a "Thermo Environmental Instruments Inc. Model 49" (UV/vis) analyser suitable

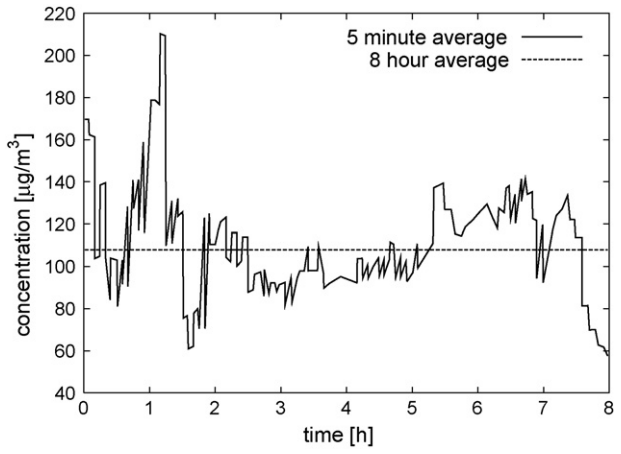

Fig. 8. Long-term concentration measurement in the vicinity of a laminating machine after installation of the new off-take. The measurements were obtained during normal production conditions. The 8 h average before the installation of the new off-take was well above 200 μg/ m^3.

for concentrations ranging from 0 to 1000 ppb. A 5 m Teflon duct (6/4 mm diameter) attached to a Teflon-membrane-filter was connected to the analyser to reach the different measurement positions.

The results of the simulations were confirmed by concentration measurements in the vicinity of the laminating machines. Table 1 shows the differences of the short term (5 min) average of reactive gas concentration. A long-term measurement was also conducted. The results are shown in Fig. 8.

5. Conclusions

A three-dimensional grid implementation was necessary to track emission paths. A careful selection of suitable boundary conditions and turbulence models proved to yield physically sensible simulation results although hardly any experimental data was accessible.

The results from the carefully implmented CFD simulations were confirmed by long- and short-term concentration measurements. Overall the concentration of reactive gas at measurement points close to the laminating machines was cut by 50%.

This research work demonstrated the applicability of recent commercial CFD code in improvement of complex industrial machinery. An important benefit of this method is the speedup of the development process and the possibility to compare different constructions without high experimental cost and without impact on the running production.

References

[1] H. Schlichting, K. Gersten, Grenzschicht-Theorie, Springer-Verlag, Berlin/Heidelberg, 1997, 9 Auflage.
[2] A. Birtigh, G. Lauschke, W.F. Schierholz, D. Beck, C. Maul, N. Gilbert, H.G. Wagner, C.Y. Werninger, CFD in der chemischen Verfahrenstechnik aus industrieller Sicht, Chemie Ingenieur Technik 72 (2000) S175–S193.
[3] Fluent, 6.2 Manual, Fluent. Inc., 2005.